

# Lawrence Berkeley National Laboratory

## Recent Work

**Title**

ISEE-C HKH HIGH ENERGY COSMIC RAYS

**Permalink**

<https://escholarship.org/uc/item/4sp701vw>

**Author**

Greiner, D.E.

**Publication Date**

1977-12-01

Submitted to IEEE Transactions on  
Geoscience Electronics

LBL-7163  
Preprint *c. 2*

RECEIVED  
LAWRENCE  
BERKELEY LABORATORY

MAR 8 1978

LIBRARY AND  
DOCUMENTS SECTION

ISEE-C HKH HIGH ENERGY COSMIC RAYS

D. E. Greiner, F. S. Bieser, and  
H. H. Heckman

December 12, 1977

Prepared for the U. S. Department of Energy  
under Contract W-7405-ENG-48

**TWO-WEEK LOAN COPY**

This is a Library Circulating Copy  
which may be borrowed for two weeks.  
For a personal retention copy, call  
Tech. Info. Division, Ext. 5716



LBL-7163  
*c. 2*

## **DISCLAIMER**

This document was prepared as an account of work sponsored by the United States Government. While this document is believed to contain correct information, neither the United States Government nor any agency thereof, nor the Regents of the University of California, nor any of their employees, makes any warranty, express or implied, or assumes any legal responsibility for the accuracy, completeness, or usefulness of any information, apparatus, product, or process disclosed, or represents that its use would not infringe privately owned rights. Reference herein to any specific commercial product, process, or service by its trade name, trademark, manufacturer, or otherwise, does not necessarily constitute or imply its endorsement, recommendation, or favoring by the United States Government or any agency thereof, or the Regents of the University of California. The views and opinions of authors expressed herein do not necessarily state or reflect those of the United States Government or any agency thereof or the Regents of the University of California.

## ISEE-C HKH High Energy Cosmic Rays

D. E. Greiner, F. S. Bieser, and H. H. Heckman  
Lawrence Berkeley Laboratory and Space Sciences Laboratory  
Berkeley, California 94720

### Scientific Aspects

The motivation of this experiment is to understand the origin of the flux of high energy cosmic rays. The contribution this experiment will make is a comprehensive measurement of the isotopic abundances ( $^1\text{H}$  to  $^{64}\text{Ni}$ ) of the cosmic ray flux near earth. To demonstrate the relevance of such an isotopic measurement we will trace, in a highly qualitative fashion, the flux from the source to the observation point near earth.

SOURCE: If the abundances and energy spectra of all isotopes produced in the source were known, then we could try various source models and see if we could identify a unique source or set of sources. There are nucleosynthesis models<sup>1</sup> which predict the source isotopic abundances which have relatively few free parameters. Thus a knowledge of as many as possible of the isotopic fluxes from the source can be used to pick between source models. In this respect the Fe group elements are particularly sensitive indicators.<sup>2</sup>

We consider the source flux to be conceptually represented by a matrix  $S_{A,Z}(E,t)$ , whose elements are labeled by A and Z, each element containing the energy and time dependence of its labeled isotope. Actually, the time dependence here is assumed to be quite small as we observe the integral of the flux over many sources and times. We will now follow this flux toward earth and see in a qualitative fashion how it is modified by the processes which take place.

ACCELERATION: The cosmic rays must be accelerated to relativistic energies. This acceleration can take place during creation or after an appreciable delay.<sup>3</sup> Whatever process is responsible for the acceleration, we know the E dependence of the  $S_{A,Z}$  will change. There are other effects which change the magnitude of the  $S_{A,Z}$  even to the extent of removal of certain isotopes. As an example, consider the isotopes produced in the source which decay solely via electron capture. They

are stable once they are stripped and at high velocity; however, they will decay during a delay between formation and acceleration. Such isotopes are called "source clocks" and are sensitive to the density of material near the source and in the interstellar region, e.g.  $^{56}\text{Ni}$  (6.1 D),  $^{55}\text{Fe}$  (7.6 Y),  $^{53}\text{Mn}$  (2 MY),  $^{44}\text{Ti}$  (47 Y). The point is that, after acceleration, the relative abundances have changed. Knowledge of the electron capture and loss cross sections, time of delay, and the electron density along the path are needed to determine the changes in relative abundance. If we represent the acceleration phase by a symbolic operator,  $A$ , which does the proper mixing and energy changes to our source flux, then the new composition after acceleration is  $AS_{A,Z}(E,t)$ .

PROPAGATION: Once up to relativistic velocities, the cosmic rays spend on the average as long a 16 million years<sup>4</sup> moving through the interstellar medium. During this flight the flux is altered by fragmentation. This is a major alteration to the relative abundances. In order to predict the effect of the propagation phase, one uses a model of propagation which will typically contain parameters such as the average time of travel and the density of the interstellar medium. The most important ingredients of the model are the relative fragmentation cross sections. In general terms, the propagation can be represented by an operator  $P$  which uses the model and cross sections to predict how the cosmic rays break up and thus enhance lower  $A$  fluxes. Long-lived isotopes such as  $^{10}\text{Be}$  (1.6 MY),  $^{26}\text{Al}$  (.88 MY),  $^{36}\text{Cl}$  (.31 MY) are called "secondary clocks. Their production and loss in the propagation process make their abundance quite sensitive to the time of travel. We are now approaching the solar system and have a flux  $PAS_{A,Z}$ .

MODULATION: As the cosmic rays approach the solar system we expect their rigidities to be altered by interaction with the solar fields and wind. Indeed, the flux does vary in time and is correlated to the solar cycle. However, the spatial extent of this variation is still unknown. Hopefully, missions traveling

to large distances from the sun (MJS) or high solar latitudes (OOE) will provide conclusive results regarding solar modulations of cosmic rays.

The mixing of isotopes may be low in the modulation process as we integrate over the entire energy spectrum of each isotope. The uncertainty comes from the fact that some, perhaps appreciable, amount of flux fails to penetrate the solar system to the observation point. Representing the modulation by the operator  $M$ , we now have the observable flux:

$$F_{A,Z} = M P A S_{A,Z}$$

### Discussion

What we see is what we get after a major alteration of the source flux. The goal is to measure  $F_{A,Z}$  and solve for  $S_{A,Z} = A^{-1}P^{-1}M^{-1} F_{A,Z}$ . To invert this equation, reliably, a detailed knowledge of  $F_{A,Z}$  is essential. The effects of  $M$ ,  $P$ , and  $A$  are quite model dependent. Given a choice of models and measured  $F_{A,Z}$ , one must determine the most consistent set of models and parameters in order to arrive at  $S_{A,Z}$ .

The more measured parameters one has to over-determine the problem the better the chances are of finding an unambiguous solution.<sup>5</sup> A comprehensive measurement of the cosmic ray isotope abundances over a wide range of elements is a major contribution to the attempt to understand the origins of the cosmic rays. The description of an instrument designed to perform these measurements follows.

### Flight Hardware

OVERVIEW: Isotopic identification of cosmic rays that come to rest in a stack of silicon detectors can be accomplished through a careful analysis of the energy loss in each of the detectors.<sup>6</sup> Our ten-element "telescope" shown in Figure 1 also includes three x-y pairs of proportional drift chambers to provide

trajectory information and a plastic scintillator surrounding the detector stack. The energy-averaged geometrical factor is  $12.9 \text{ cm}^2 \text{ str}$ .

For each event, the signals from all Si(Li) detectors are pulse-height analyzed; the drift times (and, hence, the location) in all six chambers are digitized. This data, together with various housekeeping information, is telemetered to ground stations for recording and subsequent computer analysis at LBL.

**SENSORS:** The lithium-drifted silicon detectors used in this telescope are some of the largest, most uniform ever produced. They were fabricated at LBL from 5 mm thick, two-inch diameter wafers of silicon from Topsil (Denmark). Special lapping, planer etching, and re-lithiating techniques were developed to produce detectors having an active area of  $15 \text{ cm}^2$  with a thickness uniformity better than  $\pm 10$  microns, and essentially zero dead layer ( $> 4.5 \text{ Mev}$  from  $^{241}\text{Am}$  alphas through the "dead layer" side).<sup>7</sup> Thickness uniformity was verified by scanning both surfaces with a digitized microscope. Uniformity of response to penetrating heavy ions was verified by mapping pulse-height versus position using a 480 Mev/A Argon beam from the Bevalac.

To correct for the increase in apparent detector thickness for cosmic rays entering the telescope at wide angles, an array of position sensitive detectors is used to measure the angle of incidence. Single wire proportional drift chambers were selected for use since they are inherently more rugged than multiwire chambers, less massive than hodoscopes of solid state or plastic detectors, and lend themselves to a convenient solution to the problem of delta-ray production by relativistic heavy ions.<sup>8</sup>

Figure 2 shows how 8  $\mu\text{m}$  Kapton film was bonded to epoxy-glass frames and folded to form each single axis drift space. Maximum drift lengths for the three x-y pairs are 15, 12, and 10 cm. The field-forming electrodes are 1 mm gold strips etched in a staggered pattern on both sides of the Kapton. A thick-film

resistive divider network establishes a uniform drift gradient (on both sides of the Kapton) of 300 v/cm. The double-sided staggered pattern makes each chamber surface electrostatically opaque, allowing all six chambers to be installed in one housing and thereby sharing a common gas volume. An 80 cc x 500 PSI reservoir tank and two-stage pulsed regulator system provide gas replenishment (not flow through) to compensate for leaks in the electrical feedthroughs and window O-ring seals. Lifetime at the measured leak rate is 6 years.

EVENT ENCODING: Assuming the system is not already busy, an event is encoded whenever a particle penetrates the drift chambers and at least the first two silicon detectors. As discussed in a later section, the particular detectors and chambers used for this trigger logic are all selectable by ground command. The drift chamber time to digital converters are started by the fast coincidence of the silicon detectors. The ten pulse-height analyzers begin after the chambers complete the coincidence trigger logic (The PHA's are dual-gain 4096 channel systems covering 0 to 500 Mev with a resolution of 125 kev and 500 Mev to 10 Bev in 2 Mev steps.). Flag bits are latched to indicate the presence of signals from the plastic scintillator and the "stop" detector (command selectable—usually #10). A 24 bit time-of-event register, 7 bit live timer, 12 bit scaler, and command-status-verification bits are added to the 10 thirteen-bit PHA words and 6 nine-bit TDC words to form a 256 bit page for each encoded event.

EVENT CLASSIFICATION--BUFFER MEMORY: Since the most interesting events ( $Z > 2$  that stop in the stack) are outnumbered by protons, alphas, and high-energy particles that exit the telescope, we make better use of our severely limited telemetry rate (30 bps) by classifying each event and applying a priority scheme to enhance the number of "stopping heavy ion" events telemetered while maintaining a sampling of all other types for flux normalization.

Type 1 events (highest priority) are characterized by the absence of signals



in the plastic scintillator and the "stop" detector, and a pulse height  $\geq 120$  Mev (command adjustable) in at least one of the silicon detectors. Space permitting, these events are loaded directly into a 16 event deep buffer memory for transmission by the spacecraft telemetry system. If this buffer is full, the "type one scaler" is incremented by one and the last event is over-written with the more recent one. In this way, nearly all the isotopically identifiable cosmic rays within our geometry factor can be telemetered.

Type 2 events include protons and alphas that stop in the telescope. Type 3 events are heavy ions that exit the telescope, but do not hit the plastic scintillator. The signature of a type 3 event is a pulse height  $> 27$  Mev (command adjustable) in the trigger detectors and a signal in the "stop" detector. Type 4 events are low Z (1, 2) particles that exit the telescope (no scintillator) while type 5 events are heavy ions that include a signal from the plastic scintillator (to sample the interactions in the silicon).

Single event memory buffers are available for each of the last four event types. If and when the type 1 buffer becomes empty, one of these four lower priority events is shifted into it to maintain a non-empty condition. A sequencer provides an even mixture of event types thus shifted. As with the type 1 events, old events not yet telemetered are overwritten with more recent ones (of the same type) and the appropriate scaler is incremented (until it gets read out and reset). Transmission of any event type, including the high priority type 1's, can be suppressed by ground command.

**REDUNDANCY AND COMMANDABILITY:** The inherent redundancy of a multi-element detector telescope is preserved by providing a separate PHA system for each detector. By isolating the bias supply to each detector, and providing for ground command selection of the triggering elements, the experiment can survive the loss of several detectors. Similarly, only four of the six drift chambers are necessary to determine the trajectory of incident cosmic rays. Sources of a single point failure

are further reduced by having redundant digital subsystems. They contain the PHA control circuitry, event classification logic, memory buffers, and command logic. Since most of the outputs are from CMOS circuits and only one system is powered on at any given time (ground selectable) many of the redundancy connections can simply be wire or-ed.

PACKAGING: The pre-amps, discriminators, and dual-range PHA for each detector are built on multilayer circuit boards using hybrid op-amps (built by Western Aerospace Labs), RCA CMOS I.C.'s and discrete components selected from the NASA GSFC Preferred Parts List. The six drift chambers have similar boards for amplification, discrimination, and time digitization. The photomultiplier tube discriminators and gas system electronics comprise the 17th analog board. Each of the two redundant digital systems contains 280 CMOS flat-packs soldered to an 11-layer printed circuit board measuring 10" x 10". Reynolds miniature HV connectors are used extensively to facilitate assembly and removal of detectors, subsystems, power supplies, etc. The instrument weighs 8.4 kg and requires 6.2 watts of power.

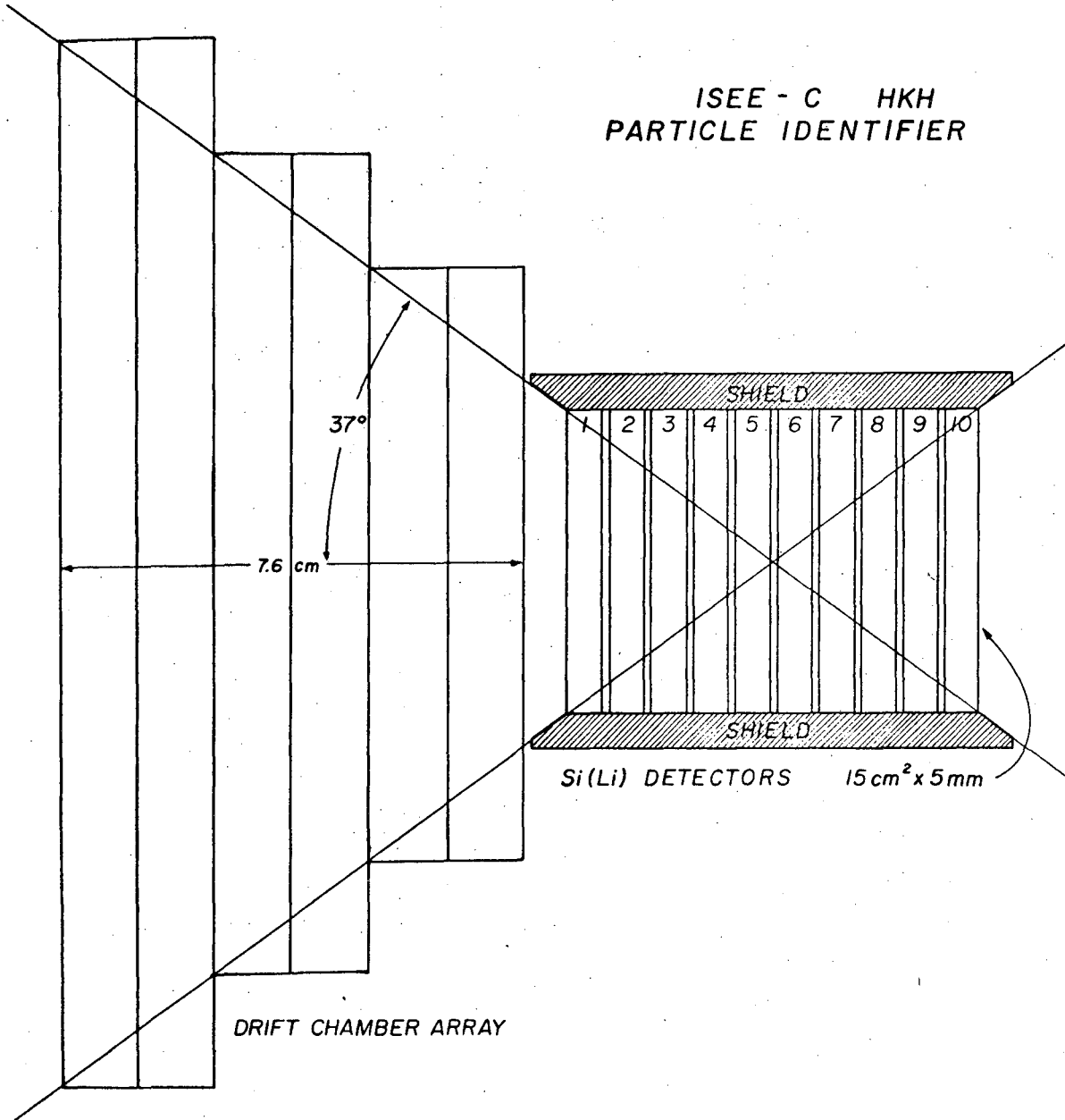
This work was done with support from the U. S. Department of Energy and National Aeronautics and Space Administration.

## Figure Captions

1. HKH particle identifier sensor array. The identifier consists of 10 lithium drifted silicon solid state detectors (.5 mm thick, 1500 mm<sup>2</sup> area) preceded by three x-y pairs of proportional drift chambers. The silicon stack is surrounded by a plastic scintillator.
2. Drift chamber construction. Field-forming electrodes etched on 8µm Kapton film form a single axis drift space. Also shown is the thick-film resistive divider network which establishes the uniform drift gradient of 300 v/cm. Six of these chambers oriented as x-y pairs form the trajectory locating sensors.

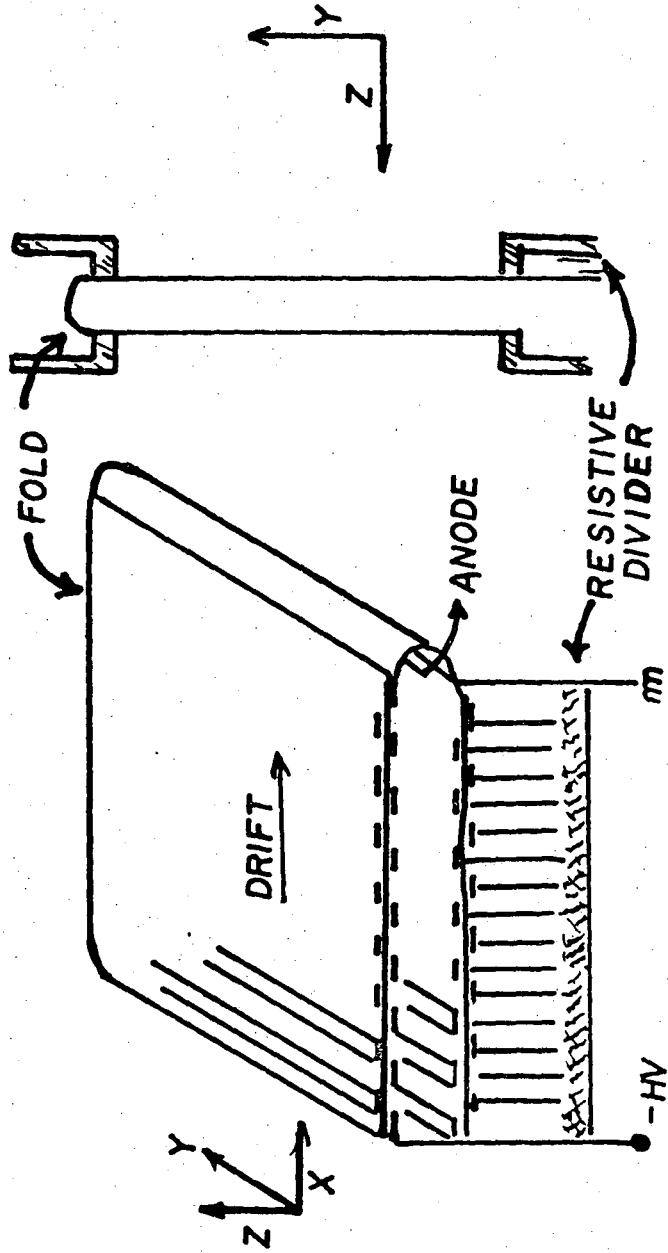
## References

1. Arnett and Clayton, Nature 227, 780 (1970).
2. K.K. Hainebach, E.B. Norman, and D.N. Schramm, Ap. J. 203, 245 (1976).
3. A. Soutoul, M. Casse, and E. Juliusson, Proc. 14th International Cosmic Ray Conference, Munich, Germany, Vol. 1, 343 (1975).
4. M. Garcia-Munoz, G.M. Mason, and J.A. Simpson, Proc. 15th International Cosmic Ray Conference, Plovdiv, Bulgaria, Vol. 1, 307 (1977).
5. M. Garcia-Munoz, G.M. Mason, and J.A. Simpson, Proc. 15th International Cosmic Ray Conference, Plovdiv, Bulgaria, Vol. 1, 301 (1977).
6. D.E. Greiner, Nuc. Inst. and Methods, 103, 291 (1972).
7. J.T. Walton, H.A. Sommer, D.E. Greiner, and F.S. Bieser, Proc. IEEE Nuc. Sci. Symposium, San Francisco (1977).
8. F.S. Bieser, D.E. Greiner, E. Beleal, and D.D. Aalami, Proc. 15th International Cosmic Ray Conference, Plovdiv, Bulgaria, Vol. 9, 91 (1977).



XBL 7711-10666

Fig. 1



XBL 778-1639

Fig. 2

This report was done with support from the Department of Energy. Any conclusions or opinions expressed in this report represent solely those of the author(s) and not necessarily those of The Regents of the University of California, the Lawrence Berkeley Laboratory or the Department of Energy.

TECHNICAL INFORMATION DEPARTMENT  
LAWRENCE BERKELEY LABORATORY  
UNIVERSITY OF CALIFORNIA  
BERKELEY, CALIFORNIA 94720